Experimental investigation of polarisation rotation in semiconductor optical amplifiers

B.F. Kennedy[a], S. Philippe[b], P. Landais[a*], A. L. Bradley[b], H. Soto[c]

a) School of Electronic Engineering, Dublin City University, Dublin 9, Ireland.

b) Physics Department, Trinity College Dublin, Dublin 2, Ireland.

c) Centro de Investigación Cientifica y de Educación Superio de Ensenada, Km. 107 Carr., Tijuana-Ensenada, Ensenada, Baja California 22860, Mexico.

* e-mail:landaisp@eeng.dcu.ie

Abstract: *In this paper we present an experimental study of polarisation rotation in a semiconductor optical amplifier. We use two techniques to investigate the gain and birefringence along the two eigen modes of the component waveguide, with and without injection. The first investigation is based on the residual reflectivity of the facet mirrors. From the modulation depth of polarisation resolved spectra, we determine the gain and the refractive indices of these modes. The second investigation takes into account the variation of the eigen mode gain and refractive indices as a function of injected power over the range –15 dBm to –3 dBm. We compare the results of these two experiments and determine that the refractive index and the single pass gain along the horizontal axis of the waveguide are higher than those along the vertical axis. Both gain and refractive index differences increase as a function of injected power in the sample under test. Furthermore we can conclude that polarisation rotation in this component is largely influenced by the power dependence of the relative gain in the TE and TM modes and birefringence.*

1. INTRODUCTION

In order to achieve all-optical signal processing, various configurations based on non-linearities in semiconductor optical amplifiers (SOAs) e.g. cross-gain modulation, cross-phase modulation and four-wave mixing have been presented [1,2,3]. Non-linear polarisation rotation (NPR) has also been demonstrated [4-6,8]. It relates to a switch of the state of polarisation of a beam injected into the device. So far considerable attention has focussed on the applications that could emerge from the NPR [6-9]. Some groups have looked at the underlying physical origins [4,7,9] but a full characterisation of the polarization change has yet to be performed, to the best of the authors' knowledge. The aim of this paper is to provide a deeper analysis of the non-linear polarization rotation in SOA by applying two different methods, which probe the polarization dependent gain and birefringence with and without signal injection. Measurements of the polarization state, as achieved using a polarimeter, provides information on the ellipticity of the output signal. Using this novel method information on the power dependence of the SOA birefringence and TE to TM gain ratio can be extracted, complementing earlier work by Manning *et al* [4]. In section 2, the experimental results are presented and discussed. In section 3, conclusions are drawn.

2. EXPERIMENTAL INVESTIGATIONS AND DISCUSSION

The SOA under test is a commercially available component. It is a 1.5-mm long bulk InGasAsP active region surrounded by InP. This structure was grown by MOCVD and it is quoted as having low polarisation dependent gain. Both facets are anti-reflection (AR) coated, with a tilted output of 12^o to reduce the Fabry-Perot resonance due to the residual reflectivity of the facets. For all the experiments the component is temperature regulated at 20^{o}C. In Fig.1 the light-output characteristic is presented. Below 220mA, the SOA acts as a LED, above this current the spontaneous emission is amplified and guided in the active region, the component acts then as an amplifier. In the inset, the emission spectrum is shown at a bias current of 400mA. It features a peak at 1574nm and a 3dB linewidth of 27nm.

We focus on two possible origins of NPR: the gain discrepancy between the eigen axes of the waveguide, and the birefringence due to different values of refractive indices for the modes. In the first experiment, these effects are investigated without injected power, providing information on the underlying properties of the waveguide. In the next experiment they are studied as a function of injected power. Both set-ups are in free space allowing optimum control and preservation of the orientation of the state of polarisation of the injected and collected signals.

2.1. Gain and birefringence in SOA without injection

The light output is collected by a 0.25 NA AR coated microscope objective; it passes through a 50 dB extinction ratio polarisation beam splitter (PBS) precisely aligned along the eigen modes of the SOA waveguide. The polarisation resolved amplified spontaneous emission (ASE) spectra are recorded for both eigen modes using a HP Optical Spectrum Analyser 86143A with a resolution of 0.07nm, as shown in Fig.2. These are referred to as TE (horizontal) and TM (vertical) in the rest of this paper. From the ASE modulation depth, introduced by Fabry-Perot resonance, we determine the wavelength dependence of the gain [11,12] and the refractive index for TE and TM. The gain reflectivity product spectrum, γ, is calculated from the formula:

$$\gamma(\lambda) = \frac{\sqrt{r(\lambda)} - 1}{\sqrt{r(\lambda)} + 1}, \qquad (1)$$

where r the modulation depth around the troughs is given by, $(P_{\max 1} + P_{\max 2})/(2\,P_{\min})$, $P_{\max 1}$ and $P_{\max 2}$ represent neighbouring peak modulation power values and $P_{\min}$ the minimum power between these peaks. γ is linked to the single pass gain, G by:

$$\gamma = \sqrt{R_1(\lambda)R_2(\lambda)}G(\lambda), \qquad (2)$$

where R_1 and R_2 are the reflectivities of the output facets. We assume that the R_1 and R_2 are equal and constant over the spectral range of our study, in accordance to reference [13]. The single pass gain is calculated from the TE and TM spectra, as shown in Fig. 2, using Eqs. (1) and (2). Our investigation was limited to bias currents above 300mA, since below this current the anti-reflection coatings and waveguide tilting minimize the ripples. Fig. 3 shows four TM and TE single pass gain spectra from 1565nm to 1595nm for bias currents of 300mA, 350mA, 400mA and 450mA. As the current increases, the peak value of the gain increases for both modes. We can note that for bias currents from 350mA to 450mA, the maximum single pass TE gain and the maximum single pass TM gain are approximately equal. There is evidence of a small dip in the TE gain spectra at 1585nm. This arises due to a decrease in the ripple modulation depth, which later recovers. It should be noted for later reference that the TE and TM gains at 1580nm under bias of 400mA are equal within error on the graph. It should be mentioned that the spectra obtained here are dependant on the value of the reflectivity. A change in these parameters will lead to a vertical shift in the spectra obtained, but would not change their profile. We can have confidence in the spectra presented in Fig. 3, the peak gain at each bias current is in agreement with the single pass gain measured as a ratio of the power out to the power in.

Birefringence has also been mentioned as an effect responsible for NPR [4,10]. In order to observe and quantify this effect, the refractive index is calculated for both the TE and TM modes. If there is a birefringent effect in the device then the period of the modulation ripples is different for both polarisations since light travels at different speeds for each mode. In other words, the ripples in the ASE spectrum goes in and out of phase with respect to each other, due to the small but finite difference in the periods of the ripple [14]. These effects can be seen in the insets of Fig. 2. Both modulations are in phase at 1577nm, however, at 1570nm they are out of phase. This means that there are different refractive indices for the TE and TM modes and there must be birefringence in the device. The refractive index is measured using the ASE spectra recorded for the gain calculations. Using the definition of the free-spectral range in a Fabry-Perot resonator, the refractive index for both modes can be calculated:

$$\Delta\lambda = \frac{2n_{g,eff}L}{k} - \frac{2n_{g,eff}L}{k+1} = \frac{2n_{g,eff}L}{k(k+1)} \approx \frac{\lambda^2}{2n_{g,eff}L}, \qquad (3)$$

where λ is the wavelength, $n_{g,eff}$ is the effective group refractive index, L is the length of the device and k is the wavevector. Using this equation we can extract $n_{g,eff}$ as a function of wavelength. $\Delta\lambda$ is the trough to trough wavelength separation, as measured from the ripples on the ASE spectra in Fig. 2 and λ is taken as the central wavelength from trough to trough. In this way a refractive index can be calculated for each central wavelength. Figs. 4(a) and (b) show the effective refractive index dependence from 1560nm to 1590nm at 400 mA for the TE and TM modes respectively. The effective refractive index is found to be 4.03 for the TE mode and 3.95 in the TM mode, where the refractive index was averaged over the complete range of wavelengths, from 1560nm to 1590nm, providing quantitative evidence of the birefringence of the device under study. These values are consistent with previously documented results [15]. Furthermore we can consider the dispersive nature of the semiconductor material and the dispersion parameter for each mode can be extracted using the following expression.

$$n_{g,eff} = n_{eff} - \lambda \frac{dn}{d\lambda} \qquad (4)$$

where $n_{g,eff}$ corresponds to the refractive index found from the free spectral range, n_{eff} is the refractive index at λ equal to zero and $\frac{dn}{d\lambda}$ the dispersive term. It is found that the scatter of the refractive index data, in Fig. 4, is too large to extract a meaningful quantitative value. However it is clear from the slope that the dispersion parameter for the TE mode is less than that of TM, in agreement with the results from [15]. Therefore the TE refractive index is higher than the TM refractive index and this difference between refractive indices decreases slightly with increasing wavelength. This birefringence is a second possible origin of the NPR in the SOA.

2.2. Gain and birefringence in SOA with injection

The experimental results discussed so far investigate possible sources of polarisation rotation due to the underlying properties of the waveguide. In order to validate the earlier results and to study the effect of the gain discrepancy and birefringence on the polarisation of an injected beam, a second set of experiments is undertaken. The ellipticity of the output amplified signal is measured as a function of the input orientation and power of a linearly polarized injected signal.

Fig. 5 shows the experimental set-up. The probe signal is provided by a tunable laser source. The polarisation of the free space signal is controlled by several components. Firstly by a polariser in order to achieve a linearly polarised signal, secondly by a half-wave plate in order to rotate the linearly polarised signal and lastly by a quarter-wave plate to compensate the mismatch between the operating wavelength of the device and the operating wavelength of the plates. The optical signal is then launched into the SOA using a 0.25 NA AR microscope objective. The launching conditions are optimised using the two mirrors and micro-control lens mount. The ASE spectrum with 2.3dBm injected power and without injected power can be seen in the inset of Fig.5. From this, we can observe a suppression of more than 6dB of the ASE indicating good injection has been achieved. A band-pass filter centred at 1580nm with a bandwidth of 10nm is placed in front of the polarimeter to reduce the influence of the random polarisation of the ASE. The polarimeter measures the ellipticity of the output signal. The ellipticity is defined as the ratio of the length of the minor axis of the polarisation ellipse by the length of the major axis. An ellipticity of zero means that the polarisation is linear. An ellipticity of -1 corresponds to circular polarisation since both lengths are equal; the negative sign is a convention to define the left-handed rotation.

The output ellipticity as a function of input orientation for a bias current of 350mA and an injection wavelength of 1580nm is shown in Fig. 6. This wavelength was specifically chosen since it corresponds to the peak gain of the TE and TM modes as shown in Fig. 3. The ellipticity is recorded for injected powers of –10dBm, -7dBm, -6dBm and –3dBm. As the injection angle increases, the ellipticity decreases, reaching a minimum at 50°, independently of input power. A minimum of –0.94 is achieved at 50° injection for -7dBm of injected power. At the minimum of ellipticity curves, the output is approaching a circular polarisation. The fact, that the minimum is reached at an angle greater than 45° indicates that the TE gain must be greater than the TM gain. For example at an input orientation of 50°, there will be more light injected into the TM mode than the TE mode and in order for the output to approach a circular polarisation the gain in TE mode must compensate for the lower injected power. The negative sign shows that the output polarisation is of left-handed rotation indicating that the TE axis is slower than the TM axis, in agreement with the result from the previous experiment with no injection. At 90° the ellipticity is zero, the linear input is injected along the TM mode, propagates and is amplified along this mode. This indicates that there is no modification of the principal axes over this power range.

In order to develop a more quantitative understanding of the experiment, we have written a model based on a propagating electric field, $\vec{E}$, having two components aligned along the modes of the waveguide.

$$\vec{E} = e^{i(\omega t - kz)}(\vec{E}_{0TE}e^{i\phi_{TE}} + \vec{E}_{0TM}e^{i\phi_{TM}}) \qquad (5)$$

where, $\vec{E}_{0TE(TM)}$ is the $\vec{E}$ component along the TE (TM) direction and its phase is $\phi_{TE(TM)}$. E_{TE} and E_{TM} are expressed as:

$$\begin{cases} \vec{E}_{0TE} = \rho E\cos(\theta)\vec{u}_{TE} \\ \vec{E}_{0TM} = E\sin(\theta)\vec{u}_{TM} \end{cases} \qquad (6)$$

where, ρ is the ratio of the single pass gain in the TE mode by the one in the TM, θ is the input angle and $\vec{u}_{TE(TM)}$ is the unit vector along the horizontal (vertical) axis. The amplitude E of the input field is taken to be unity in our model. The phases ϕ_{TE} and ϕ_{TM} are defined as follows:

$$\phi_{TE} = \frac{2\pi L n_{TE}}{\lambda} \text{ and } \phi_{TM} = \frac{2\pi L n_{TM}}{\lambda} \qquad (7)$$

As shown in Fig. 6, our numerical results fit well the experimental data using only two parameters ρ and the phase difference, $\Delta\phi = \phi_{TM} - \phi_{TE}$. The ellipticity as a function of orientation is fitted using only one value of ρ and $\Delta\phi$ for each injected power. Fig. 7 illustrates their power dependences. Within the range of injected power, the gain ratio increases up to a value of XXX for an injected power YYYY. Indicating that the single pass TE gain becomes increasingly greater than the single pass TM gain. As the injected power is decreased to zero, ρ converges towards 1 indicating the single pass TE gain approximates to the single pass TM gain. This is consistent with the results of Fig. 3, where the gain spectra are obtained under conditions of no injection.

The phase difference $\Delta\phi$ is negative demonstrating that n_{TE} is larger than n_{TM}. As the injected power is increased, the difference between the TE and TM refractive indices increases non-linearly. For future studies the polarimeter data can be considered more reliable as there are no assumptions made in the fitting, unlike the facet reflectivity in the gain spectrum analysis. However, this approach is limited since only relative gain values can be extracted. Furthermore, due to the agreement between the two methods, we can have confidence in the gain spectra of Fig. 3.

3. CONCLUSIONS

We investigated the origin of the non-linear polarisation rotation in semiconductor optical amplifiers, using two techniques. Two phenomena were considered as sources of the NRP: the asymmetric gain between the TE and TM and the birefringence. In the first experiment, there is no injected signal, allowing for the underlying properties of the waveguide to be probed. Polarisation resolved ASE spectra were recorded and the gain and refractive index for the two eigen modes of the SOA waveguide were calculated. It was found using this method, that a difference in the refractive indices of the two modes could be determined, with that along the TE axis greater than that along the TM axis. Furthermore estimations of effective refractive indices of the two modes could be extracted. The values obtained are in agreement with literature.

A new approach has been developed to investigate the gain and refractive index differences of the two eigen modes. The change in polarisation state of an injected signal at the output of the device is measured using a polarimeter. From the fit of the experimental results, with a basic electric field propagation model, we are able to measure the TE and TM gain ratio and the birefringence as a function of injected power. It is found that even though the TE and TM gains are close under low optical injection, consistent with the gain extracted from the analysis of the ASE spectra, the difference in gain between the two mode increases with increasing injected power. A higher refractive index for the TE axis compared to that of the TM is confirmed, in agreement with the spectral measurements. The birefringence is also seen to increase with increasing injected power?

Acknowledgement

This work is supported by Enterprise Ireland under the Research Innovation Fund and S. Philippe would like to thank the Irish Research Council for Science, Engineering and Technology for its support.

REFERENCES

[1] Asghari, M., White, I.H., and Penty, R.V.: 'Wavelength conversion using semiconductor optical amplifiers,'IEEE Journal of Lightwave Tech., 1997, 15, (7), pp.1181-1190.

[2] Pastor, D., Martinez, A., Capmany, J., Sales, S., Ortega, B., and Munoz, P.: 'Experimental characterization of XGM-SOA-Based wavelength converted SCM systems', IEEE Photonics Tech. Letters, 2003, 15, (1), pp 114-116.

[3] Lee, S-L., Gong, P-M., and Yang, C-T.: 'Performance enhancement on SOA based four-wave mixing wavelength conversion using an assisted beam', IEEE Photonics Tech. Letters, 2002, 14, (12), pp 1713-1715.

[4] Manning, R.J., Antonopoulos, A., Le Roux, R., and Kelly, A.E.: 'Experimental measurement of nonlinear polarization rotation in semiconductor optical amplifiers', Electronics Lett., 2001, 37 (4), pp 229-231.

[5] Soto, H., Erasme, D., and Guekos, G.: 'Cross polarization modulation in semiconductor optical amplifiers,' IEEE Photon. Technol. Lett., 1999, 11, pp. 970–972.

[6] Patrick, D.M., Ellis, A.D., Davies, D.A.O., Tatham, M.C., and Sherlock, G., 'Demultiplexing using polarization rotation in a semiconductor laser amplifier,' Electronic Letters, 1994, 30, (4), pp 341-342.

[7] Liu, Y., Hill, M.T., Tangdiongga, E., de Waardt, H., Calabretta, N., Khoe, G.D., and Dorren, H.J.S.: 'Wavelength conversion using nonlinear polarization rotation in a single semiconductor optical amplifier', IEEE Photonics Tech. Letters, 2003, 15, (1), pp 90-92.

[8] Stephens, M.F.C., Asghari, M., Penty, R.V., and White, I.H.: 'Demonstration of ultrafast all-optcal wavelength conversion utilizing birefringence in semiconductor optical amplifiers', IEEE Photonics Tech. Letters, 1997, 9, (4), pp 449-451.

[9] Dorren, H.J.S., Lenstra, D., Liu, Y., Hill, M.T., and Khoe, G.: 'Nonlinear polarization rotation in semiconductor optical amplifiers: theory and application to all-optical flip-flop memories', IEEE. Journal of Quantum Electronics, 2003, 39,(1), pp 141-148.

[10] Soto, H., Dominguez, J.C., Erasme D., G. Guekos,: 'Demonstration of an all-optical switch using cross-polarization modulation in semiconductor optical amplifiers', Microw. and Optic. Technol. Lett., 2001, 29, (3), pp. 205-209.

[11] Hakki, B., and Paoli, T., 'Gain spectra in GaAs double-heterostructure injection lasers', Journal of Applied Physics, 1975, 46, (3), pp 1299-1306.

[12] Guekos

[13] Meritt, S.A., Dauga, C., Fox, S.,Wu, I.-F., and Dagenais, M.,: 'Measurement of the facet modal reflectivity spectrum in high quality semiconductor travelling wave amplifiers', Journal of Lightwave Technology, 1995, 13, (3), pp 430-433.

[14] Diez, S., Schimt, C., Ludwig, R., Weber, H.G., Doussiere, P., Duceiller, T.,: 'Effect of birefringence in bulk semiconductor optical amplifier on FWM', IEEE Photonics Tech. Letters, 1998, 10, (2), 212-214.

[15] Guekos, G., "Photonic devices for telecommunications", Editor Springer-Verlag, 1999, pp 144-145.

Figure Captions

Fig 1: L-I characteristic of the SOA under test. Insert: ASE spectrum at 400mA.
Fig. 2:Polarisation resolved spectra. Insert: Ripples in phase and out of phase.
Fig. 3: Polarisation resolved gain spectra for I=300mA, 350mA, 400mA and 450mA. TE (▲) and TM (o).
Fig. 4: Refractive index dependence on the wavelength at I=350 mA for (a) the TE mode and (b) the TM mode.
Fig. 5: Experimental set-up of the injection experiment. Insert: Spectra of the ASE without and with injection.
Fig. 6: (a) Output ellipticity as a function of the angle of injection of a linearly polarised input for –10 dBm, -7 dBm -6 dBm and –3 dBm (o) represents experimental data, simulations are represented by lines.
Fig. 7: Gain ratio between TE and TM modes and phase difference as a function of input power. Lines are a guide to the eye.

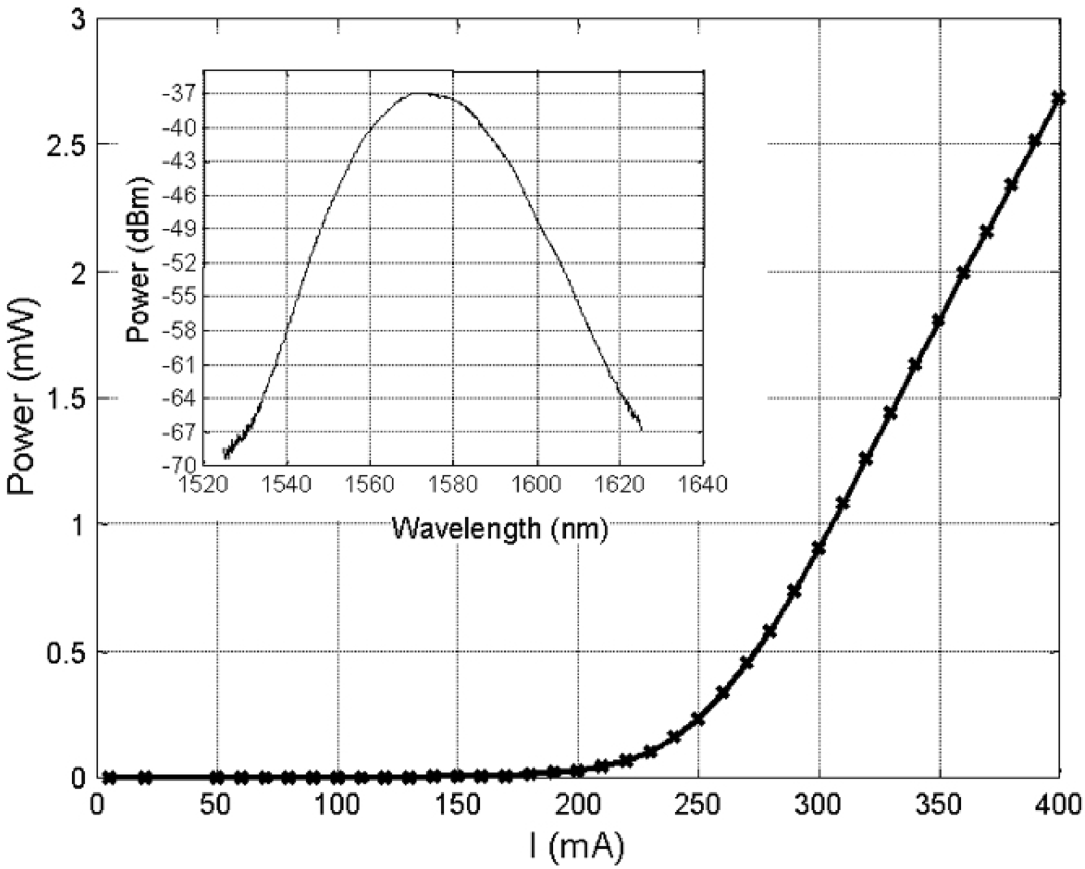

Power (mW)
I (mA)
0
0.5
1
1.5
2
2.5
3
0
50
100
150
200
250
300
350
400
Power (dBm)
Wavelength (nm)
-37
-40
-43
-46
-49
-52
-55
-58
-61
-64
-67
-70
1520
1540
1560
1580
1600
1620
1640

Fig.1

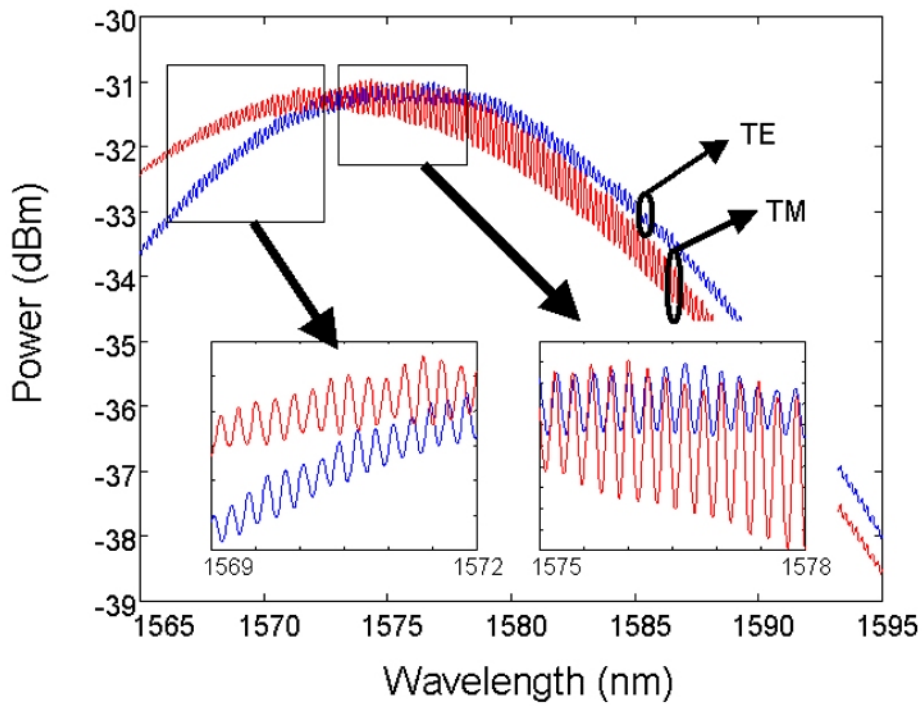

-30
-31
-32
-33
-34
-35
-36
-37
-38
-39
Power (dBm)
1565
1570
1575
1580
1585
1590
1595
Wavelength (nm)
TE
TM
1569
1572
1575
1578

Fig. 2

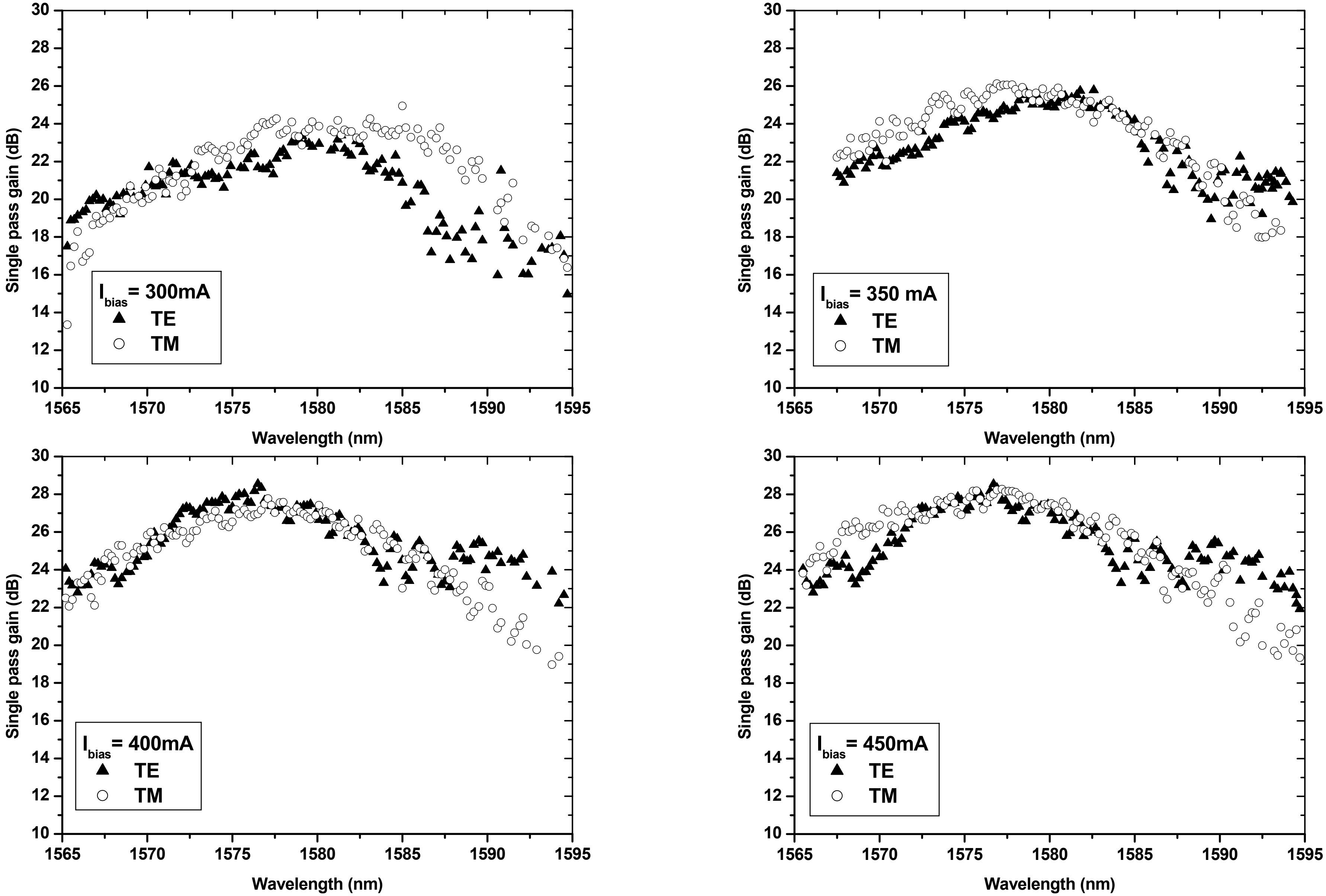
Single pass gain (dB)
Wavelength (nm)
I_bias = 300mA
TE
TM
I_bias = 350 mA
TE
TM
I_bias = 400mA
TE
TM
I_bias = 450mA
TE
TM

Fig. 3

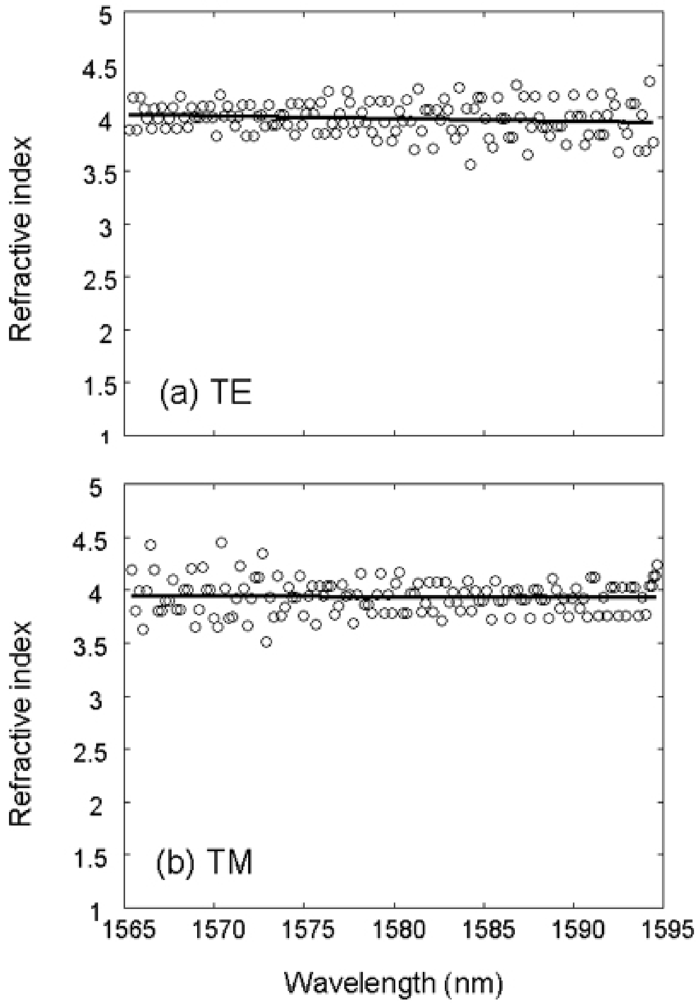

Fig. 4

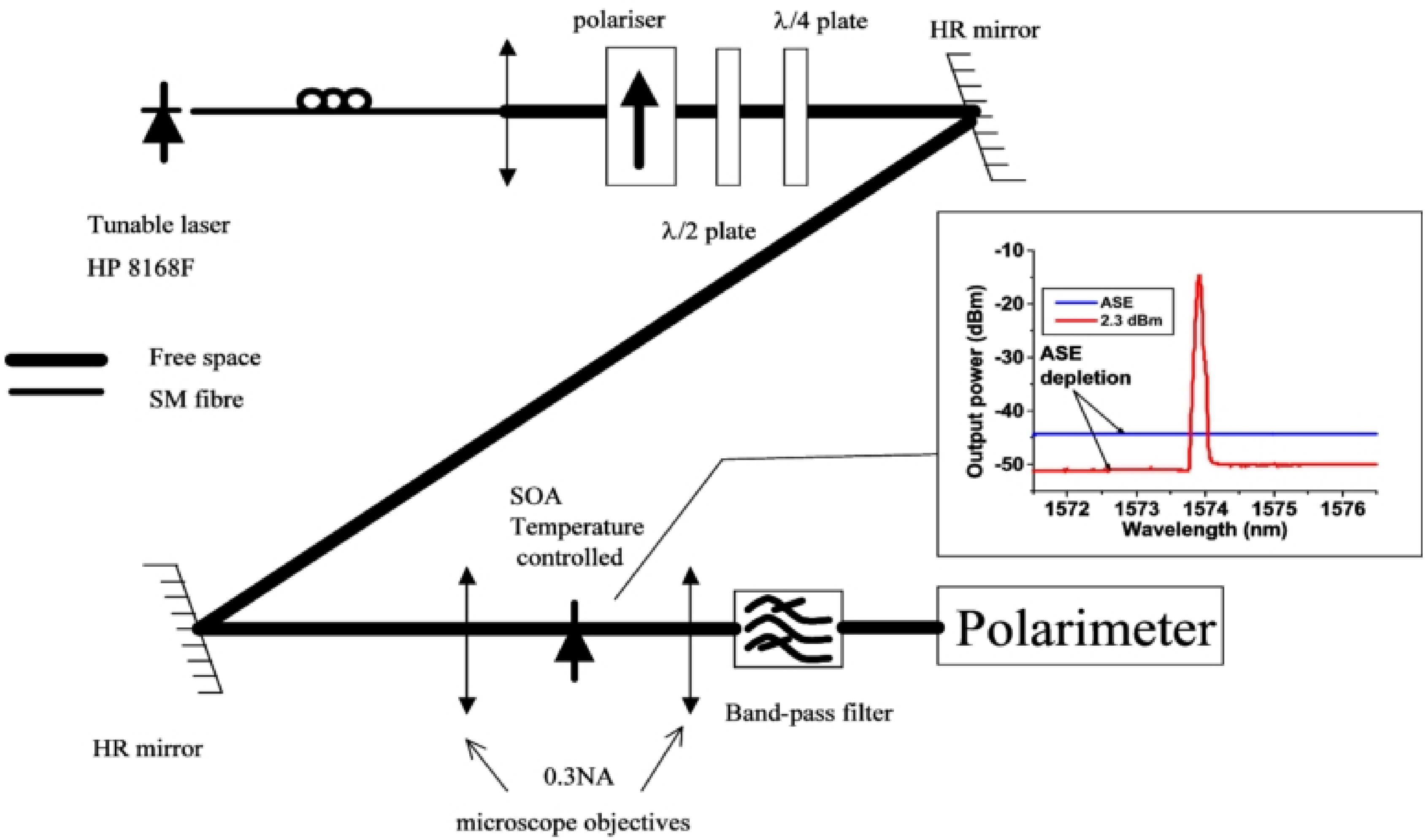
polariser
λ/4 plate
HR mirror
Tunable laser
HP 8168F
λ/2 plate
Free space
SM fibre
-10
-20
-30
-40
-50
Output power (dBm)
ASE
2.3 dBm
ASE
depletion
1572
1573
1574
1575
1576
Wavelength (nm)
SOA
Temperature
controlled
Polarimeter
Band-pass filter
HR mirror
0.3NA
microscope objectives

Fig. 5

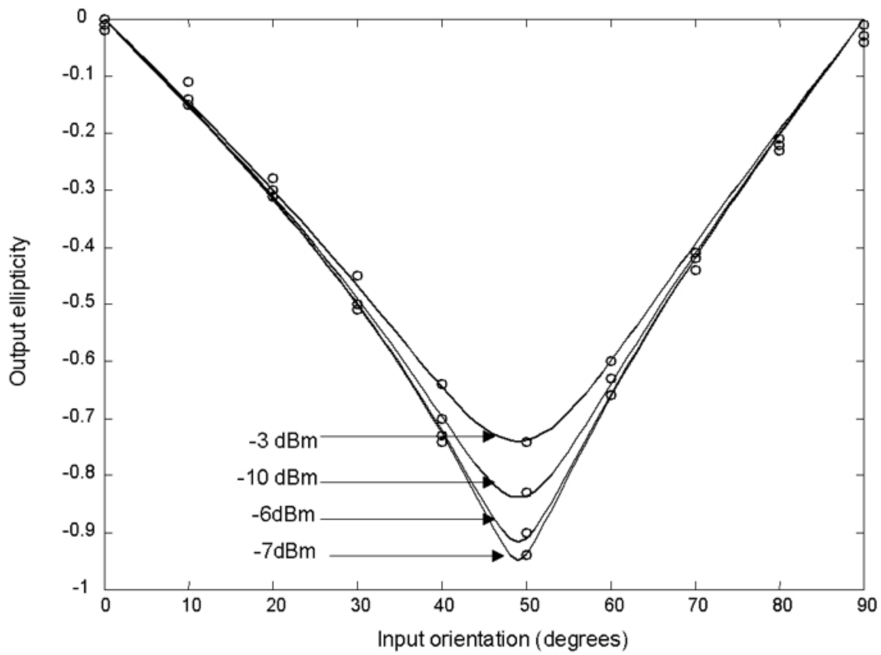
0
-0.1
-0.2
-0.3
-0.4
-0.5
-0.6
-0.7
-0.8
-0.9
-1
Output ellipticity
-3 dBm
-10 dBm
-6dBm
-7dBm
0
10
20
30
40
50
60
70
80
90
Input orientation (degrees)

Fig. 6

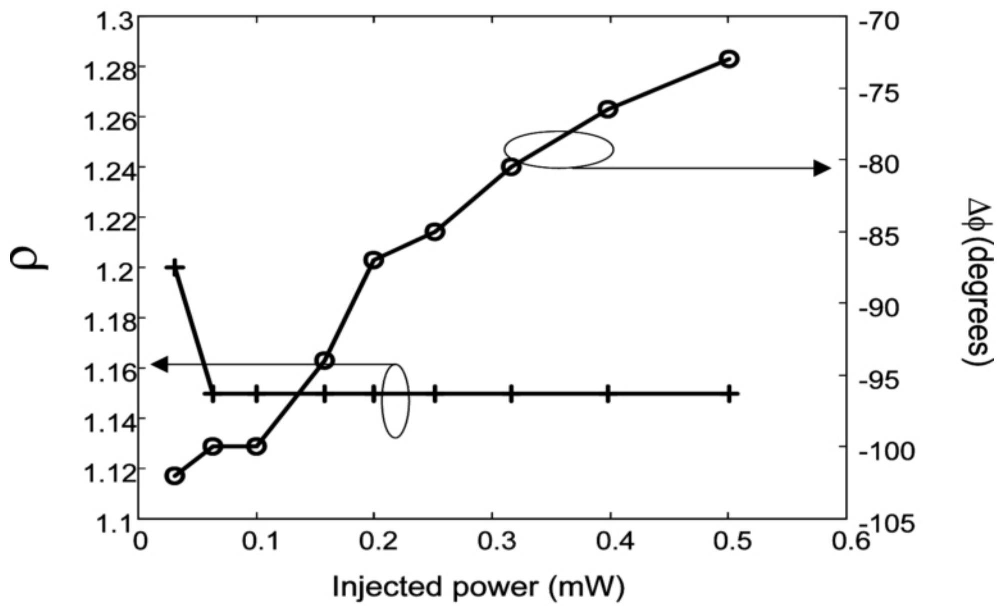

1.3
1.28
1.26
1.24
1.22
1.2
1.18
1.16
1.14
1.12
1.1
ρ
0
0.1
0.2
0.3
0.4
0.5
0.6
Injected power (mW)
-70
-75
-80
-85
-90
-95
-100
-105
Δφ (degrees)

Fig. 7